Nano Research
https://doi.org/10.1007/s12274-017-1823-9
Research Article
ISSN 1998-0124
CN 11-5974/O4

Real-time decay of fluorinated fullerene molecules on Cu(001) surface controlled by initial coverage

Andrey I. Oreshkin[1,§] (✉), Dmitry A. Muzychenko[1,§] (✉), Sergey I. Oreshkin[2], Vladimir A. Yakovlev[3], Palanichamy Murugan[4], S. Selva Chandrasekaran[4], Vijay Kumar[5,6], and Rauf Z. Bakhtizin[7]

[1] *Department of Physics, Lomonosov Moscow State University, 119991 Moscow, Russia*
[2] *Sternberg Astronomical Institute, Lomonosov Moscow State University, 119234 Moscow, Russia*
[3] *Institute of Petrochemical Synthesis, Russian Academy of Sciences, 119991 Moscow, Russia*
[4] *CSIR Central Electrochemical Research Institute, Karaikudi 630003, Tamil Nadu, India*
[5] *Dr. Vijay Kumar Foundation, 1969 Sector 4, Gurgaon 122001, Haryana, India*
[6] *Center for Informatics, School of Natural Sciences, Shiv Nadar University, NH91, Tehsil Dadari, Gautam Budh Nagar 201 314, Uttar Pradesh, India*
[7] *Department of Physical Electronics, Bashkir State University, 450074 Ufa, Russia*
[§] *Andrey I. Oreshkin and Dmitry A. Muzychenko contributed equally to this work*

Received: 29 March 2017
Revised: 29 July 2017
Accepted: 25 August 2017

KEYWORDS

fluorinated fullerene, (001) Cu surface, two-dimensional (2D) molecular island, 2D gas phase, self-assembling molecules, scanning tunneling microscopy (STM), density functional theory (DFT)

ABSTRACT

In this study, the evolution of $C_{60}F_{18}$ molecules on a Cu(001) surface was studied by means of scanning tunneling microscopy and density functional theory calculations. The results showed that fluorinated fullerenes (tortoise-shaped polar $C_{60}F_{18}$) decay on Cu(001) surfaces by a step-by-step detachment of F atoms from the C_{60} cage. The most favorable adsorption configuration was realized when the F atoms of $C_{60}F_{18}$ pointed towards the Cu surface and six F atoms were detached from it. The results also showed that a further decay of $C_{60}F_{12}$ molecules strongly depended on the initial $C_{60}F_{18}$ coverage. The detached F atoms initially formed a two-dimensional (2D) gas phase which then slowly transformed into F-induced surface structures. The degree of contact between the $C_{60}F_{12}$ molecules and the Cu(001) surface depended on the density of the 2D gas phase. Hence, the life-time of fluorinated fullerenes was determined by the density of the 2D gas phase, which was affected by the formation of new F-induced structures and the decay of $C_{60}F_{12}$ molecules.

Address correspondence to Andrey I. Oreshkin, oreshkin@spmlab.phys.msu.su; Dmitry A. Muzychenko, mda@spmlab.ru

1 Introduction

During the past few decades, organic materials have gained popularity as important components of molecular nanoelectronic devices [1–5]. In particular, the most abundant fullerenes, C_{60}, with their unique cage-like structure and electron-accepting nature have fascinated researchers. Their properties make them a promising material for the development of electro-active elements for photovoltaic solar batteries and dynamic layers for thin film transistors [6, 7]. The stable derivatives of fullerenes, namely, endohedral and exohedral (such as fluorinated fullerenes) possess many attractive properties suitable for diverse applications owing to their higher electron affinity as compared to their non-fluorinated forms [8, 9]. Fluorination is a powerful technique to tune the electronic and optical properties of fullerene molecules by stabilizing the energy levels of their frontier orbitals [10, 11]. The family of known exohedral fluorinated fullerenes consists of tens of identified compositions of $C_{60}F_n$ with n = 18–48 for the most isolated derivatives [12–16] and even up to n = 60–102 for experimentally observed hyperfluorinated fullerenes [17, 18].

The ability of fluorinated fullerenes to effectively attach electrons and form stable anions is the reason for their application as molecular p-dopants for the production of hydrogen-terminated diamonds [19–21] and epitaxial graphene surfaces [22]. Moreover, the charge-transfer doping of semiconductor materials by fluorinated fullerenes has been studied to form ultra shallow junctions on Si to suppress the short channel effect and decrease leakage current in miniaturized metal oxide semiconductors [23]. The high reactivity of fluorinated fullerenes allows their use as dopants for achieving p-type conductivity in pentacene, which is used in the manufacture of organic light-emitting Schottky diodes [8]. Recently, because of the development of new organic materials compatible with Si-based semiconductor technology, the microscopic studies of the physical and electronic properties of $C_{60}F_n$ molecules adsorbed on semiconductor surfaces [24–27] have gained attention. In an organic field-effect transistor, an increase in the electron affinity of fluorinated fullerenes causes a decrease in the electron injection barrier at the interface between the molecular film [28] and the metal electrode [9, 29]. A successful implementation of organometallic device architectures requires a detailed study of their nanoscale morphology as well as electronic properties such as the molecule-metal band alignment and interfacial charge transfer. Owing to its fascinating physical (high electric dipole moment $\boldsymbol{d}$ > 9 Debye) and geometric (18 F atoms bound to only one hemisphere of C_{60} cage) properties, the tortoise-shaped polar $C_{60}F_{18}$ [15, 16] is the most attractive material among fluorinated fullerenes for the growth of thin organic films on metal surfaces. A detailed study of the structural and electronic properties of thin films of fluorinated fullerenes (in particular $C_{60}F_{18}$) adsorbed on metal surfaces is therefore considered to be essential for further advances in the development of organic nanoelectronics. Nevertheless, until now only a limited number of studies [28, 30, 31] have been dedicated to this problem. Moreover, the role of metal substrates in the adsorption process of fluorinated fullerenes as well as the stability of fluorinated fullerenes on metal surfaces is still unclear.

Here, we report the first-time observation of the evolution and real-time decay of $C_{60}F_{18}$ molecules on a Cu(001) surface. The results showed that the growth of fluorinated fullerene molecules is a multiple stage process where the coverage extent of the molecules plays a crucial role in the formation of ordered surface nanostructures. Our room temperature scanning tunneling microscopy (STM) experiments combined with first-principles calculations revealed that when $C_{60}F_{18}$ was deposited on a Cu(001) surface, six F atoms showed a tendency to detach from the adsorbed molecules. The detached F atoms formed a 2D gas phase on the Cu(001) surface when the initial molecular coverage exceeded 0.5 monolayer (ML). The existence of the 2D gas phase prevented the contact of the $C_{60}F_{12}$ molecules with the Cu(001) surface and a further loss of F atoms, providing a prolonged life-time of fluorinated fullerene on the Cu(001) surface. These results shed light on the complex surface processes occurring during the formation of the self-assemblies of fullerene molecules through adsorption. Hence, these results would prove to be useful for applications such as nanoscale-localized chemical reactions and organometallic nanoelectronics.

2 Methods

2.1 Experimental

All STM measurements were carried out with an ultra-high vacuum (UHV) (with a base pressure of about 4 × 10^{-11} mbar) STM setup (Omicron Nanotechnology) at room temperature using W tips. The tips were cleaned *in situ* by repeated flashing well above 1,800 K in order to remove the surface oxide layer and additional contamination. The tip quality was routinely checked by acquiring atomic-resolution images of the Cu(001) surface (see Fig. S1 in the Electronic Supplementary Material (ESM)). STM topography imaging was carried out in a constant current mode. Everywhere in the text the tunneling bias voltage V_t refers to the sample voltage. The STM tip was virtually grounded. Image processing was done using Nanotec WSxM [32].

A single crystal of Cu(001) (99,9999% purity) was cleaned under a UHV condition by repeated cycles of Ar^+ sputtering at 1 keV and annealing at 820 K for 2–3 h leading to the formation of wide (about 500 nm) defect-free terraces separated by monoatomic steps (Figs. S1(a) and S1(b) in the ESM).

$C_{60}F_{18}$ molecules were deposited on a clean Cu(001) surface at room temperature using a Knudsen cell. The pressure during the deposition was 1.8 × 10^{-10} mbar. A deposition rate of 0.03 ML/min was used in all the experiments. Here 1 ML is defined as the number of molecules forming a close-packed monolayer of fluorinated fullerene on the Cu(001) surface.

2.2 Computational details

The structural and electronic properties of fluorinated fullerene molecules on the Cu(001) surface were studied using density functional theory (DFT) functions implemented in the Vienna *ab initio* simulation package [33, 34]. The electron–ion interactions were represented using the projector augmented wave pseudopotential method [35]. The exchange and correlation energies were calculated using the generalized gradient approximation (GGA) method [36]. A cut-off of up to 400 eV was used for the plane wave kinetic energies to expand the wave function and structural optimization. A 6×6 surface supercell was constructed from a unit cell of the (001) Cu surface. The Cu surface was modeled with three layers to accommodate 108 Cu atoms in the supercell. One $C_{60}F_{18}$ molecule was deposited on the Cu(001) surface within this supercell. The Brillouin zone of the supercell was sampled with the Γ-point for the ionic optimization. Self-consistent field calculations were carried out until the absolute value of force on each ion reduced to less than 10 meV/Å.

3 Result and discussion

Two-dimensional (2D) islands of fullerene molecules with ordered structure were realized as a result of the deposition of the $C_{60}F_{18}$ submonolayer on the Cu(001) surface at room temperature without thermal annealing. The intriguing aspect of this observation is the formation of two different types of self-assembled molecular islands depending on the extent of coverage. The first type of molecular islands comprised of only pure C_{60} molecules on the Cu(001) surface and were obtained when the $C_{60}F_{18}$ molecular coverage did not exceed 0.3 ML. The islands of the second type consisted of the fluorinated fullerene molecules and could be achieved when the molecular coverage was more than 0.5 ML. Indeed, Fig. 1(a) shows a well-known close-packed structure of C_{60} molecules with a (10,6)×(0,4) surface unit cell. The formation of a regular and ordered monolayer film having a striped structure oriented along the [010] or [100] directions with two distinct molecular configurations is attributed to the missing row reconstruction of the underlying Cu surface [37]. The imaging height of the observed molecular structure was estimated from the surface profile *aa′* shown in Fig. 1(c). It was found to be 6.8 ± 0.3 Å (6.2 ± 0.3 Å) for the bright (dim) species. The STM topography results were in good agreement with the results of previous studies [37] in which the adsorption of C_{60} molecules on Cu(100) was studied by means of STM and X-ray photoelectron diffraction. The small discrepancy in the height of the C_{60} island obtained by us in this study and that reported previously [37] (a difference of ~0.4 Å) can be explained by the tunneling bias dependence of the molecule height in the STM topography images. A detailed analysis of the experimental high-resolution STM

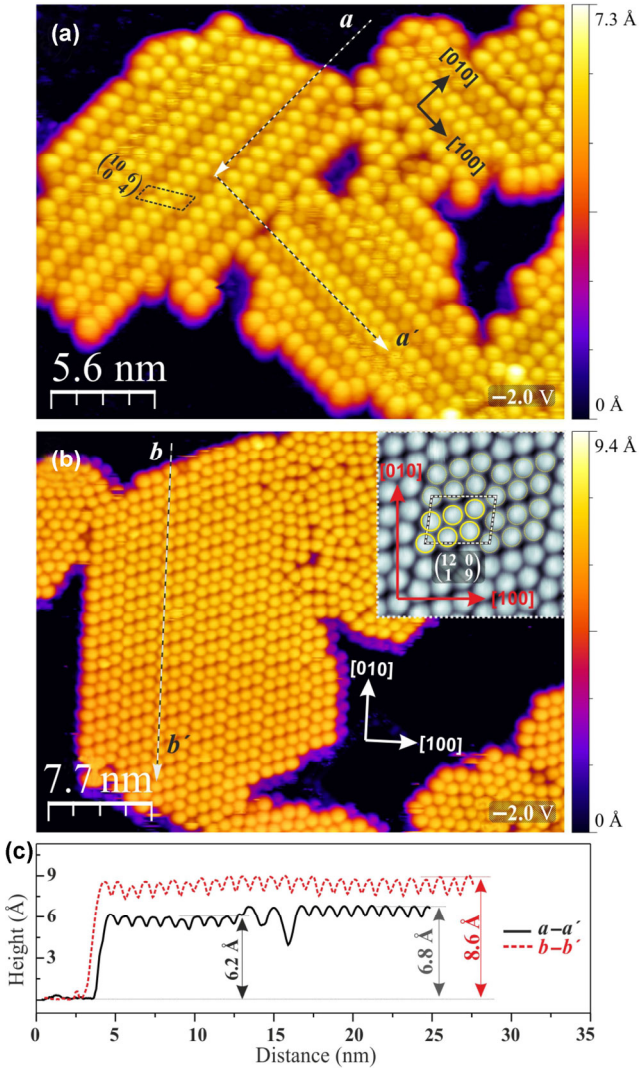

Figure 1 Self-assembled 2D molecular islands formed as a result of $C_{60}F_{18}$ deposition on the Cu(001) surface. (a) STM topography image of the C_{60} molecular island formed on the Cu(001) surface at a molecular coverage of 0.28 ML. (b) STM topography image of the islands of fluorinated fullerenes formed on the Cu(001) surface at a molecular coverage of 0.5 ML. Inset: close-up view of the fluorinated fullerenes packing order (12,0)×(1,9). (c) Height profiles taken along the dashed arrows *aa′* and *bb′* indicated in (a) and (b), respectively. The (10,6)×(0,4) and (12,0)×(1,9) surface unit cells are indicated by dashed and black rectangles in (a) and by black and white parallelograms in the inset of (b), respectively. The unit cell (12,0)×(1,9) consisting of six fluorinated fullerene molecules indicated by yellow circles in the inset of (b). The main crystallographic directions and the tunneling voltage V_t are indicated for each image. Tunneling current I_t was 30 pA.

topography images (see Fig. S7 in the ESM) reveals that the molecules observed within the 2D islands were same as pristine C_{60} molecules.

Figure 1(b) shows the second type of self-assembled 2D molecular islands which were obtained at higher coverages (> 0.5 ML). The structure of these 2D islands changed drastically as compared to the 2D islands consisting of C_{60} molecules. First, the fullerenes within the 2D islands aligned by the height, and the dim and bright rows that are typical for the growth of C_{60} molecules on Cu(001) surfaces disappeared. The imaging height of the 2D molecular islands in this case became higher and was found to be 8.6 ± 0.3 Å (Fig. 1(c)). Second, the self-assembled molecular arrangement within the 2D islands also changed. Instead of close-packed molecules with a (10,6)×(0,4) surface periodicity, a few types of metastable structures could be observed within the 2D islands. The evolution of these packing structures depended on the time elapsed after the deposition of $C_{60}F_{18}$ molecules on the Cu(001) surface. Initially, a (12,0)×(1,9) packing structure was predominant. This structure then transformed into a hexagonal (4,2)×(0,4) structure with the same height before finally converting into the well-known C_{60} (10,6)×(0,4) packing structure (see below for more details). The second type of islands were initially formed by the fluorinated fullerene molecules which slowly decayed on the Cu(001) surface over time and finally resulted in the formation of pure C_{60} 2D molecular islands. The decay rate of fluorinated fullerene molecules on Cu(001) surfaces is mainly determined by the initial $C_{60}F_{18}$ coverage and can vary from a few minutes to several days.

In order to understand the dynamics of $C_{60}F_{18}$ decay on the Cu(001) surface, a series of DFT-based *ab initio* calculations were carried out for different orientations of $C_{60}F_{18}$ molecules relative to the substrate (Fig. 2(a)) within a supercell. Taking into account the complicated structure and strong asymmetry of $C_{60}F_{18}$ molecules, three different orientations were studied: (i) the F atoms in $C_{60}F_{18}$ molecules pointing towards the surface (model (1) in Fig. 2(a)), (ii) $C_{60}F_{18}$ molecules oriented sideways (model (2) in Fig. 2(a)), and (iii) F atoms in $C_{60}F_{18}$ molecules pointing out of the surface (model (3) in Fig. 2(a)). The calculations showed that the equilibrium configuration with the lowest energy was realized when the F atoms in the $C_{60}F_{18}$ molecules were pointing towards the surface (model (1) in Fig. 2(a)) and six F atoms were detached from the

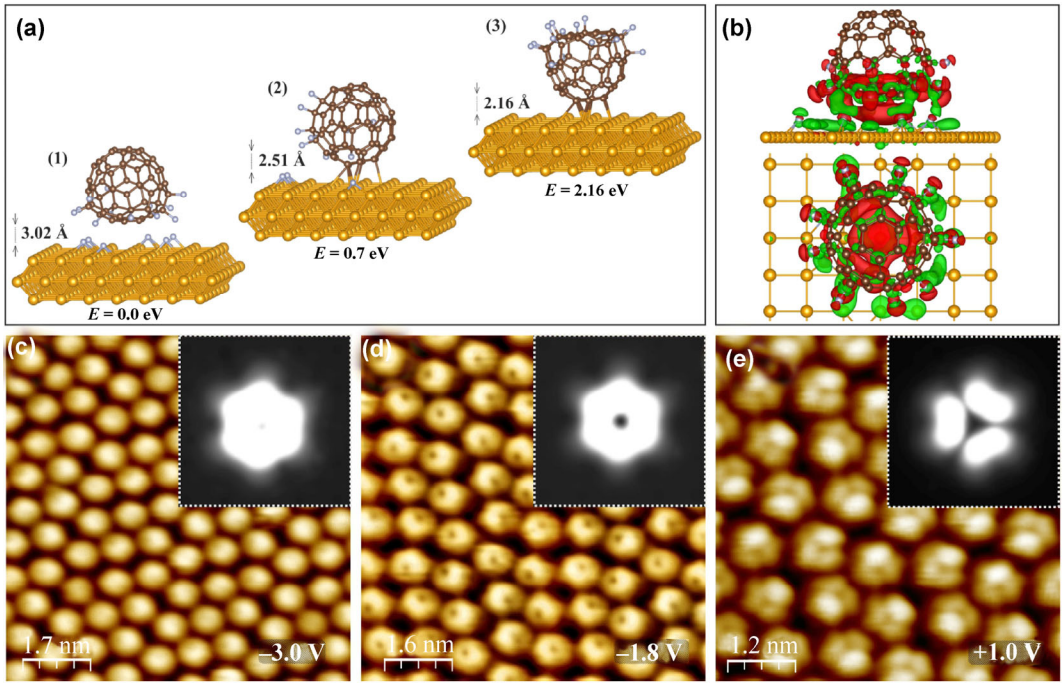

Figure 2 (a) Calculated atomic structures of three different orientations of $C_{60}F_{18}$ molecules adsorbed on a Cu(001) surface. The surface is represented by a three-layer slab with a supercell containing 108 Cu atoms. The energies are given with respect to the lowest energy (stable) configuration (1) in which the fluorine atoms point towards the surface. The distance between the adsorbed molecule and the surface is also indicated. (b) The excess and depletion of charge $\Delta\rho = \rho^{Cu(001):[C60F12+6F]} - \rho^{Cu(001):C60F12} - \rho^{Cu(001):6F}$ are shown for configuration (1) of the absorbed molecule on the Cu(001) surface. For clarity both the side and top views (upper and bottom images, respectively) are given. Red (green) color isosurface (value 0.005 $e^{-}/Å^3$) represents excess (depletion) of charge after the adsorption. There is excess charge around the F atoms and a deficiency of charge between the molecule and the surface. (c) and (d) High resolution filled-state and (e) empty-state STM topography images of the fluorinated fullerene molecular film on Cu(001). The corresponding calculated filled-state images are shown in the insets of (c) and (d) and empty-state image in the inset of (e) based on model (1) shown in (a). The tunneling voltage V_t is indicated for each experimental and calculated image (c)–(e). The tunneling current I_t was 20 pA.

original fluorinated fullerene molecule: $C_{60}F_{18}/Cu \rightarrow C_{60}F_{12}/Cu + 6F^{-}/Cu$. The height of the $C_{60}F_{12}$ molecule above the Cu(001) surface in this case was more than that in the case of model (2) where the $C_{60}F_{18}$ molecules were oriented sideways. The $C_{60}F_{12}$ molecule lied on the detached F atoms on the Cu(001) surface. We carried out the calculations of a $C_{60}F_{12}$ molecule on a fully F-covered Cu(001) surface with 18 F atoms in a supercell. The adsorption energy was negligible (actually very weakly repulsive within GGA due to the repulsion between F on C_{60} and F on the Cu(001) surface). Therefore, it can be stated that $C_{60}F_{12}$ was loosely bonded to the partially F-covered surface during the adsorption of $C_{60}F_{18}$ on the Cu(001) surface. This weak interaction also suggests the possibility of the migration of the $C_{60}F_{12}$ molecule on the Cu(001) surface (see Fig. S5 in the ESM) with further a detachment of F atoms at low coverages. The binding energy of a F atom on the Cu(001) surface was calculated to be 4.21 eV, which is in good agreement with the value reported previously (4.22 eV) [38]. However, this value is significantly higher than 3.50 eV per F atom when 18 F atoms are adsorbed on a C_{60} fullerene. Therefore, the detachment of F atoms from fluorinated fullerenes is energetically favorable (as was found in our study).

In the case when $C_{60}F_{18}$ molecules were oriented sideways (see model (2) in Fig. 2(a)), three F atoms left the molecule and interacted with the surface. The energy of this configuration was 0.7 eV higher than that of configuration (1). The binding energy of the $C_{60}F_{15}$ molecule together with the three F atoms on the Cu(001) surface was found to be 1.64 eV higher than that of a free $C_{60}F_{18}$ molecule. The relaxed

configuration of the molecule shown in model (3) of Fig. 2(a) was least favorable. In this case all the F atoms in the $C_{60}F_{18}$ molecule were pointing out of the surface and did not interact with the Cu(001) surface. The energy of this configuration was 2.16 eV higher than that of configuration (1).

The distances between the fluorinated fullerene molecule and the Cu(001) substrate for configurations (1)–(3) were found to be 3.02, 2.51, and 2.16 Å, respectively (see Fig. 2(a)). The largest distance was obtained for configuration (1). This is because in this case, the fluorinated fullerene molecule had an indirect contact with the Cu(001) surface, which is evident from the appearance of detached F atoms over the surface in this case. Such atoms were not observed in configurations (2) and (3) where a C–Cu bond was formed with a typical bond lengths 2.1 and 2.2 Å, respectively (similar to C_{60} on a Cu(001) surface). This result is in accordance with the general tendency that the surface profile above fluorinated fullerene molecules from STM image is higher than for the profile above C_{60} molecules on Cu(001) surface, as shown in Fig. 1(c). Moreover, the difference between the heights of fluorinated fullerene and C_{60} monolayer-thick islands increases if the missing row reconstruction of the underlying Cu surface in the case of C_{60} island is taken into account [37].

Figure 2(b) shows the difference in the charge densities of the combined system ($C_{60}F_{12}$ molecule + 6F on Cu(001) surface) and the sum of the charge densities of $C_{60}F_{12}$ molecule + 6F alone and the Cu(001) surface. Two views (side view in the upper image and top view in the lower image) are shown where the isosurfaces shown in red and green colors represent the excess (positive difference) and depletion (negative value of the difference in charge densities) of charge, respectively. The isosurface value of the charge density was taken to be 0.005 $e^-/Å^3$. These results show that there was an excess charge on the $C_{60}F_{12}$ molecule near the F atoms and a depletion of charge (polarization charge) occurred at the interface between the molecule and the surface.

Finally, we verified the proposed piecemeal decay of $C_{60}F_{18}$ molecules by modeling the electronic properties of $C_{60}F_{12}$ on the Cu(001) surface, i.e., by obtaining the corresponding STM constant current topography images. The simulated STM images were obtained by Tersoff–Hamann approximation [39, 40] while maintaining a distance of 2 Å between the STM tip and the top point of the molecule. Figures 2(c)–2(e) show a series of filled and empty-state experimental and calculated (see insets in Figs. 2(c)–2(e)) STM constant current topography images of fluorinated fullerene molecules on the Cu(001) surface. All the images for configuration (1) were obtained when the F atoms were pointing towards the surface. The images for configurations (2) and (3) are shown in Fig. S2 in the ESM. The filled-state STM images (Figs. 2(c) and 2(d)) of the $C_{60}F_{12}$/Cu(001) system show regular arrangements of bright spots with an average distance of 10.3 Å between them. In the filled-state image, some dark points could be clearly observed on these bright spots at tunneling bias voltages V_t in the range of −1.5 – −2.2 V both for the experimental and the calculated images (Fig. 2(d)). On the other hand, for the lower tunneling bias voltages (V_t < –2.2 V) no dark points were observed (Fig. 2(c)). The empty-state STM images show a trefoil arrangement (Fig. 2(e)) which is in good agreement with the calculated STM images (see inset in Fig. 2(e)). Based on the calculated images the appearance of the dark points in the filled-state (Fig. 2(d)) images and trefoils in the empty-state images (Fig. 2(e)) can be directly attributed to the top hexagon ring and three upper pentagon rings of the $C_{60}F_{12}$ molecule, respectively. However, it should be noted that for the experimental images (Figs. 2(d) and 2(e)) some asymmetry of the individual fluorinated fullerene molecules could be clearly observed. In the filled-state STM topography images (Fig. 2(d)), the dark points on bright spots shifted from the center to different directions, while in the empty-state STM topography images (Fig. 2(e)) one lobe of the trefoils was always more intense than the other two in contrast to the calculated images where a centrosymmetric structure of $C_{60}F_{12}$/Cu(001) was obtained both for the filled and empty-state regimes. These discrepancies can be attributed to the fact that in the constructed model of $C_{60}F_{12}$/Cu(001), the directionality of molecules was not taken into account because of the nearest-neighbor interactions between the adsorbed molecules in the real 2D fluorinated fullerene molecular islands on the Cu(001) surface. The fluorinated

fullerene molecules were arranged in the form of a monolayer film and were subjected to two competitive interactions: the molecule–substrate and molecule–molecule interactions. In order to maintain a balance between these interactions, the molecules tended to move to find optimum adsorption sites because of very low adsorption energies. Because of such a low adsorption energy, the molecules could rotate to achieve the best packing order within the 2D molecular islands. These results clearly show that the most favorable arrangement of $C_{60}F_{18}$ molecules on a Cu(001) surface is the one in which F atoms point towards the surface. The results also show that the interaction leads to the detachment of F atoms from fluorinated fullerene molecules.

The DFT calculations showed that the F atoms detached from the $C_{60}F_{18}$ molecule formed a buffer layer between $C_{60}F_{12}$ and the Cu(001) surface. At the same time, the magnitude of the adsorption energy of the chemisorbed F atoms on the densely packed metal surface decreased with an increase in the coverage because of the presence of repulsive lateral electrostatic interactions. This phenomenon resulted in the formation of an atomic gas phase on the surface [41, 42]. At high $C_{60}F_{18}$ molecular coverages (> 0.5 ML), the partially decayed fluorinated fullerene molecules were supported by the F-atom gas phase, leading to a decrease in the molecule–substrate interaction. Thus, the $C_{60}F_{12}$ molecule–molecule interaction appears to have a crucial role during the growth of monolayer films. The interaction among the strongly asymmetric $C_{60}F_{12}$ molecules with high dipole moments gave rise to an angular momentum which resulted in their inclination i.e. the deviation of their dipole moments from the normal direction to the surface (see inset in Fig. 3(a)). The analysis of the positions of the specific dark points in the filled-state STM (Figs. 2(d) and 3(a)) images showed that the inclination of the $C_{60}F_{12}$ molecules involved changes in both the polar (θ) and azimuthal (φ) angles (see inset

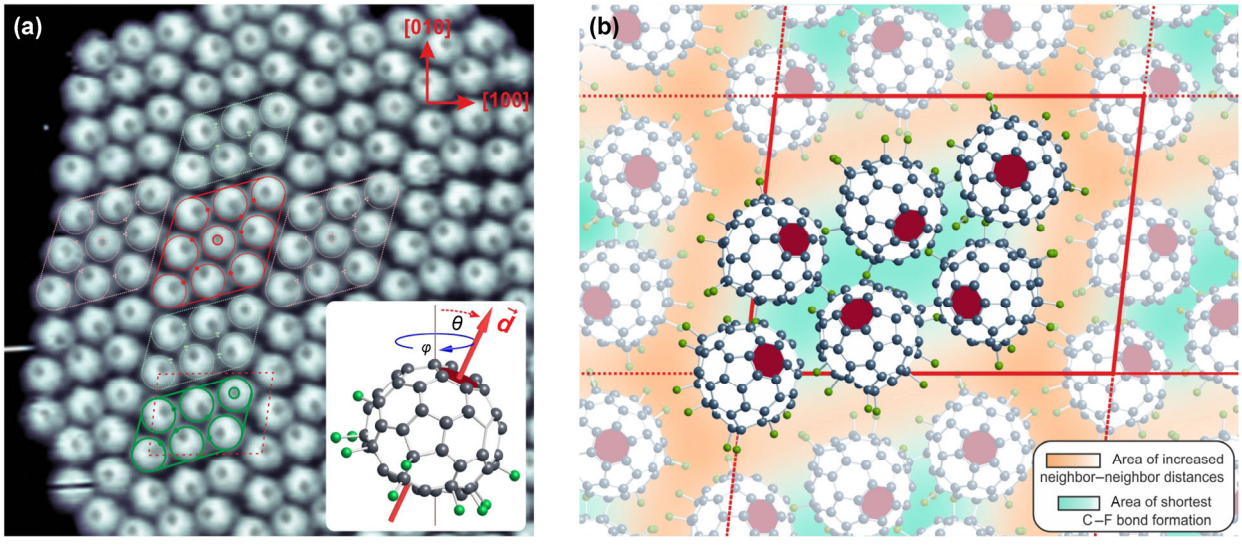

Figure 3 The precession of the dipole moment ***d*** of $C_{60}F_{12}$within the (12,0)×(1,9) packing order molecular island. (a) A high-resolution filled-state STM topography image (V_t = –1.8 V, I_t = 18 pA) of a $C_{60}F_{12}$ molecular island on the Cu(001) surface exhibits specific dark points on bright spots which are shifted in various directions because of the precession of the dipole moments of the individual $C_{60}F_{12}$ molecules. The (12,0)×(1,9) surface unit cell is indicated by a dashed red parallelogram. The orientations indicate groups of six (green outline) and nine (red outline) $C_{60}F_{12}$ molecules with deterministic pattern of dark point displacement (see text for more details). The inset shows the deviation of the dipole moment ***d*** (red arrow) of the individual $C_{60}F_{12}$ molecules from the normal to the surface (vertical black axis) directions with a change in both the polar (θ) and azimuthal (φ) angles. (b) The ball-and-stick model of the $C_{60}F_{12}$ molecules packed within the (12,0)×(1,9) surface unit cell (red parallelogram) where the dipole moment ***d*** of each molecule is oriented in such a way that the top hexagon (dark-red solid filled hexagon) is shifted in different directions to fit the pattern in the green parallelogram shown in (a). Orange-white gradient color indicates the area of increased neighbor–neighbor distances because of the formation of intermediate C–F bonds and the presence of F–F Coulomb repulsive interactions, while the blue-white gradient region represents the area of the formation of shortest C–F bond between six neighboring $C_{60}F_{12}$ molecules.

in Fig. 3(a)). A visible displacement of the specific dark points in the range of six $C_{60}F_{12}$ molecules (green solid outline in Fig. 3(a)) within the (12,0)×(1,9) surface unit cell (red dashed line parallelogram in Fig. 3(a)) created a strictly deterministic pattern (see Figs. S3(a) and S3(b) in the ESM for more details). Moreover, in the case of violation of the local order, the appearance of new domains consisting, for example, of nine $C_{60}F_{12}$ molecules (red solid outline in Fig. 3(a)) could be observed. The packing order of this structure also had a strictly deterministic pattern. The exceptions from this deterministic pattern can be attributed to the boundaries of the 2D islands (see Figs. S3(a) and S3(b) in the ESM).

Figure 3(b) shows a ball-and-stick model of $C_{60}F_{12}$ molecules packed within a (12,0)×(1,9) surface unit cell (red solid line parallelogram) where the dipole moment ***d*** of each molecule was oriented in such a way that the top hexagon (dark red solid fill) is shifted in different directions in order to fit the pattern observed in the experimental STM image (see solid green outline in Fig. 3(a)). The tilt of the dipole moment of $C_{60}F_{12}$ caused the F atoms to be oriented sideways at one side of the molecule and in the downward direction at the other side (see inset in Fig. 3(a) and Figs. S3(c) and S3(d) in the ESM). The equilibrium configuration within the group of six $C_{60}F_{12}$ molecules was realized when most of the F atoms were pointing outside the group, resulting in minimal Coulombic F–F repulsive interactions between the nearest neighbors and the formation of the shortest C–F contacts [16] between the neighboring $C_{60}F_{12}$ molecules (Fig. 3(b)). This mechanism of energy minimization also explains the close-packing structure inside the group of six $C_{60}F_{12}$ molecules and increased distances between the groups because of the repulsive F–F Coulombic interactions. Indeed, the appearance of well-separated boundaries between the groups of six $C_{60}F_{12}$ (Figs. 1(b), 2(c)–2(e), and 3(a)) molecules is in good agreements with the proposed model. Here, it should be noted that the inclination of $C_{60}F_{12}$ molecules within 2D islands can cause additional detachment of F atoms from the $C_{60}F_{12}$ molecules. As it has been shown above, the F atoms in contact with a Cu surface prefer to leave the C_{60} cage. Therefore, in the tilted $C_{60}F_{12}$ molecules (see inset in Fig. 3(a)), an extra loss of a few F atoms might have occurred. Thus, strictly speaking, 2D molecular islands consist of $C_{60}F_n$ molecules with different number of F atoms ($n \leq 12$). Initially, the value of n was close to 12, however, it decreased with time and eventually became 0.

To further provide the experimental evidence for the existence of the atomic gas phase on the Cu(001) surface and to elucidate the mechanisms controlling the rate of decay of fluorinated fullerenes, other typical changes occurring on the Cu(001) surface after the adsorption of $C_{60}F_{18}$ should be considered. The STM topography images showed that unlike the clean Cu(001) surface (prior to the $C_{60}F_{18}$ adsorption, (Fig. S1 in the ESM)), the $C_{60}F_{18}$-adsorbed Cu(001) surface showed a drastic appearance of "telegraph noise" [43] immediately after the $C_{60}F_{18}$ adsorption (Fig. 4(a)). We could not achieve an atomic resolution in the noisy area of the Cu(001) surface. However, the 2D molecular islands were not affected by the "telegraph noise". Therefore, the "telegraph noise" was exclusively intrinsic to the Cu(001) surface and was independent of the STM tip conditions. The appearance of this "telegraph noise" can be attributed to the hopping of F atoms in the tunneling gap. Similar phenomena of the coexistence of solid 2D islands and 2D molecular gas phase for SubPc molecules on an Ag(111) surface [44, 45] as well as the existence of a 2D gas phase of alkali metals on a Si(111) surface [46, 47] have been reported previously. Figure 4(a) shows that a 2D gas phase was present on the Cu(001) surface regardless of the $C_{60}F_{18}$ coverage. An increase in the molecular coverage lead to a significant increase in the 2D gas phase density (i.e. the density of the noisy streak pattern on the STM images). On the basis of our calculated data, it can be stated that the source of the gas phase on the Cu(001) surface was the decayed $C_{60}F_{18}$ molecules, which had a tendency to lose 3–6 F atoms even at the first contact with the surface (Fig. 2(a)).

The formation of new surface structures (see labels 1–3 in Fig. 4(b)) created by F could be observed approximately 15 h after the deposition of $C_{60}F_{18}$ on the Cu(001) surface. Three types of new structures were observed: (1) a $(\sqrt{17}\times\sqrt{17})R14°$ surface phase (label 1 in Fig. 4(b)); (2) c(2×2) subsurface phase (label 2 in Fig. 4(b)), and (3) $(2\sqrt{2}\times\sqrt{2})R45°$ surface phase (label 3 in Fig. 4(b)). The nucleation of these new structures

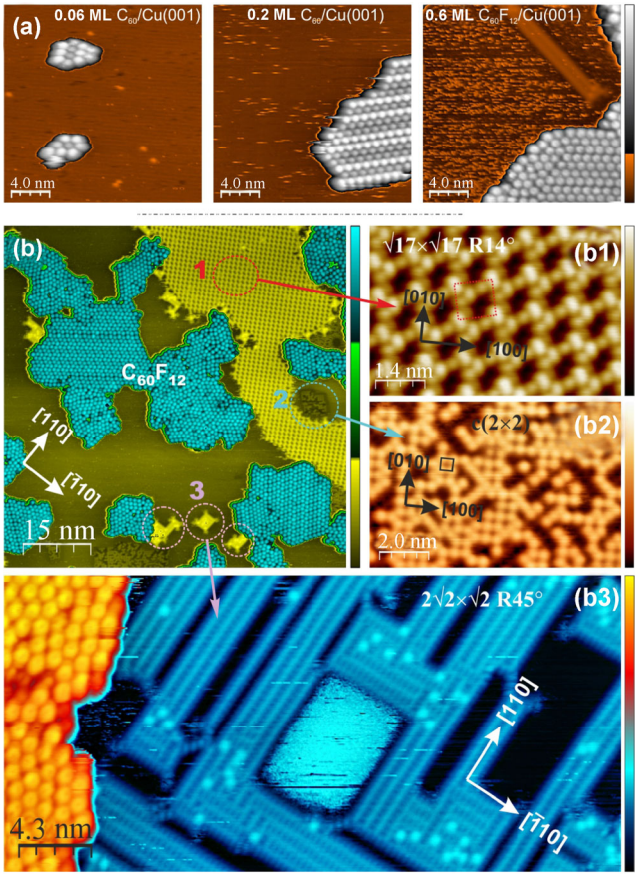

Figure 4 Fluorine-related 2D gas phase and its 2D condensed phases on the Cu(001) surface induced by $C_{60}F_{18}$ decay. (a) STM topography images (V_t = –2.0 V, I_t = 26 pA) of Cu(001) surface subjected to different coverage of $C_{60}F_{18}$ molecules: 0.06, 0.2, and 0.6 ML from left to right, respectively. The "telegraph noise" on the STM images associated with the 2D gas phase drastically increased with an increase in the coverage. (b) Large-scale STM topography images of new surface structures (indicated by 1–3) induced by the growth of a 2D gas phase over time: (1) (√17×√17)R14° surface phase (denoted as 1 in (b)); (2) c(2×2) subsurface phase (denoted as 2 in (b)) and (3) (2√2×√2)R45°-F surface phase (denoted as 3 in (b)). In all the cases the tunneling voltage V_t was –1.8 V and the tunneling current I_t was 16 pA. The main crystallographic directions are indicated for the images.

occurred at a $C_{60}F_{18}$ molecular coverage of around 0.3 ML. Furthermore, at $C_{60}F_{18}$ coverages higher than 0.5 ML, the following growth features were observed: (i) The growth of the new structures began some time after the deposition; (ii) a significant growth of the structure (1) and the appearance of nucleation centers for types (2) and (3); (iii) a rapid growth of structures (2) and (3) over time and the conversion of structure (1) into (3); (iv) termination of further growth with a predominance of structure (3) (see Fig. S4 in the ESM). Structures (1) and (3) had nearly the same height of about 1.5 Å and grew on top of the Cu(001) surface, while structure (2) grew in the plane of the Cu(001) surface, i.e. the upper atomic layer of the Cu(001) surface was degraded because of an etching mechanism. It is noteworthy that the noisy features associated with the 2D gas phase still existed on the surface during the growth of the new structures. However, the noisy features were not observed in the last structure. Moreover, the "telegraph noise" decreased with the growth of the new structures and finally its traces could be found only in very limited areas. Thus, on the basis of the experimental data, we can associate the noisy streak pattern with the 2D gas phase and the new structures with the 2D condensed phase. A full understanding of the formation of F-induced new structures on Cu(001) surfaces requires a detailed investigation using DFT-based calculations, which are clearly beyond the scope of our current research.

We also calculated the interaction energy of $C_{60}F_{12}$ and $C_{60}F_{18}$ molecules with fluorinated Cu(001) surface, by considering two models: (i) with F atoms pointing towards the surface and (ii) with F atoms pointing upwards. Our calculations show that the model with F atoms pointing upwards was energetically favorable because the carbon atoms in the molecules interacted with the F atoms on the surface. In addition, in the model with F atoms pointing upwards there was repulsion between F atoms of the molecule and the F atoms on the surface (see Fig. S8(a) in the ESM). Despite the fact that the energy of $C_{60}F_{12}$ ($C_{60}F_{18}$) on the F-covered Cu(001) surface with F atoms pointing upwards was only 0.27 eV (0.74 eV), and lower than that in the case of the F-covered Cu(001) surface with F atoms pointing towards the surface, the calculated STM images agree with experimental results by considering the case of the surface in which the F atoms were pointing towards the surface (see Figs. S8(b) and S8(c) in the ESM). These results suggest that once the $C_{60}F_{18}$ molecules interacted with the Cu(001) surface, the fluorinated fullerene left after the detachment of F atoms remained oriented in the direction towards the surface. This behavior can be explained by the existence of additional molecule–molecule interactions within the 2D molecular islands, which is responsible for the maintenance of the original molecule configuration

with F atoms pointing towards the surface.

These results show that the experimental results of the 2D gas phase were in good agreement with the expectations from the DFT model of $C_{60}F_{12}$ on the Cu(001) surface. Nonetheless, to gain more insight into the phenomena of further real-time $C_{60}F_{12}$ decay, the evolution of 2D fluorinated fullerenes islands should be studied.

As we have already discussed above, the metastable (12,0)×(1,9) structure was realized because of the presence of a 2D gas phase which supported $C_{60}F_{12}$ molecules on Cu(001) to prevent its further contact with the surface and a further loss of F atoms. The weak bonding between the fluorinated fullerene molecules and the surface made them quite mobile. Therefore, the shape of the islands depended on the deformation over time (Fig. S5 in the ESM). Moreover, a saltatory movement of the fluorinated fullerenes in the tunneling gap could also be observed (see the zoomed images in Fig. S5 in the ESM). This phenomenon further confirms the presence of weak bonding between the $C_{60}F_{12}$ molecules and the Cu(001) surface.

On the basis of the above discussion, it can be stated that new structures on Cu(001) surfaces are formed because of the transformation of the 2D gas phase into a 2D condensed phase (F-related structures), leading to a decrease in the 2D gas phase density on the Cu(001) surface. Consequently, the $C_{60}F_{12}$ molecules start interacting spontaneously with the Cu(001) surface because the 2D gas density is not high enough to sustain a further existence of the metastable configuration. As a result of the spontaneous contact with the surface, the $C_{60}F_{12}$ molecules lost additional F atoms located nearest to the Cu(001) substrate, thereby maintaining a constant density of the 2D gas phase. Because of a further loss of F atoms, the fluorinated fullerenes tended to change the self-assembly packing order within the 2D molecular islands, causing a violation of the metastable (12,0)×(1,9) order and its step-by-step transformation into a close-packed hexagonal (4,2)×(0,4) structure. Figure 5(a) shows the 2D island of fluorinated fullerene molecules 70 h after the deposition. The appearance of the local ordering violation of the (12,0)×(1,9) packing structure is clearly visible and the regions of a new hexagonal (4,2)×(0,4) packing order can be observed within the white dashed counters in Fig. 5(a).

During the further continuous growth of the new structures, the 2D gas phase density remained nearly constant because of the continued decay of the fluorinated fullerene molecules. At the same time the packing order within the 2D molecular islands changed completely to a close-packed hexagonal one (Fig. 5(b1)), while the visible height of all the molecules within the 2D island remained the same as that of the $C_{60}F_{12}$ molecules (Figs. 1(b) and 1(c)). Apparently, according to the calculated configuration (1) (Fig. 2(a)) each of the $C_{60}F_{12}$ molecules was able to successively lose 12 F atoms. This might be the reason for the constant 2D gas phase density constant during the 100 h following the first nucleation of F-related structures (at a molecular coverage of 0.6 ML).

In the case when most of the F atoms left the $C_{60}F_{12}$ molecules but the growth of the new F-related structures continued, the height of the molecules decreased to 1.2 Å within the 2D molecular islands. At first this effect was predominant for singular molecules (Fig. 5(b1) and 5(b2)) with the further involvement of the groups and rows of the molecules (Fig. 5(b3) and 5(b4)). The final stage showed an avalanche-like reduction in the height of most of the molecules within the 2D island (Fig. 5(b5)) and a complete transformation of close-packed hexagonal (4,2)×(0,4) packing into the well-known (10,6)×(0,4) structure with bright and dim rows typically observed for molecular islands consisting of clean C_{60} molecules (Fig. 5(b6)). The final configuration consisting of C_{60} 2D islands and F-related structures (type (2) and (3)) in between the islands was observed 200 h after the deposition of $C_{60}F_{18}$ on the Cu(001) surface (for the molecular coverage of 0.6 ML). It should be noted that at a molecular coverage of 0.6 ML the new F-related structures covered the entire Cu(001) surface between the 2D molecular islands. In the case when the initially deposited $C_{60}F_{18}$ molecules (at coverage 0.6 ML) on the Cu(001) surface decayed completely, the fluorine coverage was 0.6 ML. These results are in good agreement with the STM image shown in Fig. 5(b6) in which the entire surface is occupied by C_{60} molecules and F-induced structures.

The dependence of coverage on the type of the molecular islands (Figs. 1(a) and 1(b)) formed can be

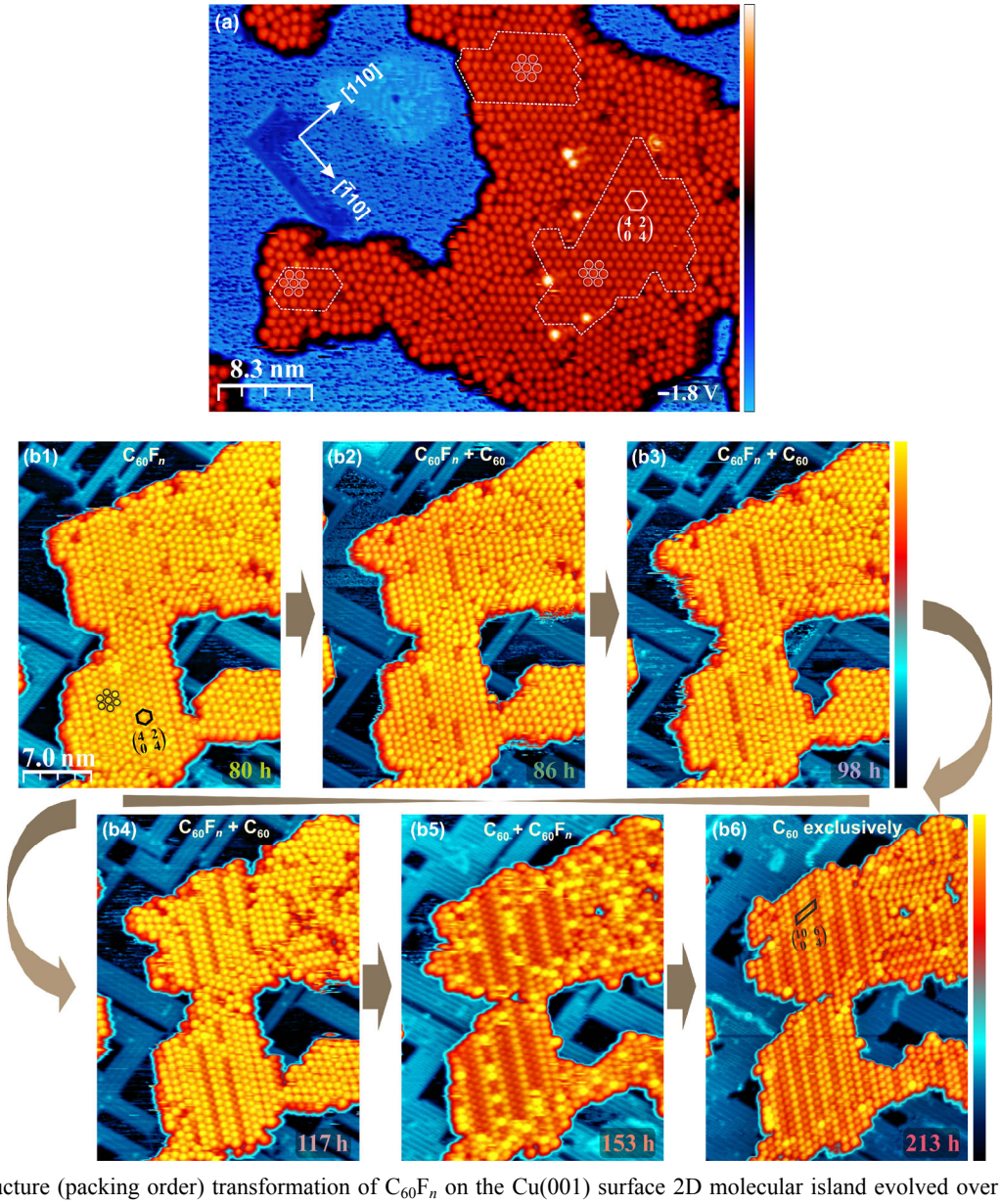

Figure 5 Structure (packing order) transformation of $C_{60}F_n$ on the Cu(001) surface 2D molecular island evolved over time. (a) STM topography image (V_t = –1.8 V, I_t = 18 pA) of 2D molecular island during the further decay of $C_{60}F_n$ molecules. The local ordering violation of the initial (12,0)×(1,9) packing structure (Fig. 1(b)) is easily distinguishable and a new hexagonal (4,2)×(0,4) packing order can be observed within the outlined areas. (b) Real-time decay of fluorinated fullerenes $C_{60}F_n$ on the Cu(001) surface. (b1)–(b6) Time-sequence series of the STM topography images of the same 2D molecular island evolved over time. The height of the molecules has a tendency to decrease step-down for random singular molecules (b1) and (b2) with the further involvement of the groups and rows of molecules (b4) and (b3). (b5) The avalanche-like reduction of height for most of the molecules. (b6) Final equilibrium configuration of the (10,6)×(0,4) phase with bright and dim rows typical for C_{60} molecules. A tunneling voltage V_t of –2.0 V and a tunneling current I_t of 12 pA were used for STM images (b1)–(b6). STM images capture time elapsed after the deposition of $C_{60}F_{18}$ on the Cu(001) surface is indicated for each STM image (b1)–(b6) in the right low corner.

elucidated by taking into account the crucial role of the 2D gas and condensed phases on the life-time of $C_{60}F_n$ molecules. At very low molecular coverages (< 0.2 ML) six F atoms were detached from each adsorbed fluorinated fullerene molecule which is apparently not enough to form a 2D gas phase. As a result, the $C_{60}F_n$ molecules lost the remaining F atoms quickly and formed C_{60} islands. The concentration of F atoms

on the Cu(001) surface was not high enough to create even nucleation points for the new F-related structures, and F atoms interacted locally with Cu(001) (see Fig. S6(a) in the ESM). In the case of higher molecular coverages (0.2–0.3 ML), the 2D gas phase was formed only because of the detachment of 18 F atoms from the first portion of the adsorbed molecules, leading to the formation of intermixed islands composed of C_{60} and $C_{60}F_n$ molecules (see Fig. S6(b) in the ESM). Then the $C_{60}F_n$ molecules continued to decay over time yielding clean C_{60} islands and a very limited area of the new F-related structures (Fig. S6(c) in the ESM).

4 Conclusion

In summary, we analyzed the real-time decay of fluorinated fullerenes on Cu(001) surfaces depending on the initial molecular coverage. The *ab initio* calculations confirmed that the most stable configuration of the molecules was realized when the F atoms in $C_{60}F_{18}$ pointed towards the surface and six F atoms detached from the original fluorinated fullerene molecule. All the calculated images for this configuration were in good agreement with the high resolution atomic STM images. When the initial coverage of the $C_{60}F_{18}$ molecules was less than 0.3 ML, all the molecules reacted with the Cu(001) surface, leading to the formation of ordered C_{60} islands surrounded by a 2D gas phase. An increase in the molecular coverage lead to a significant increase in the 2D gas phase density. The source of the gas phase on the Cu(001) surface decayed the $C_{60}F_{18}$ molecules, which showed a tendency to lose 3–6 F atoms even at the first contact with the surface. At a higher $C_{60}F_{18}$ coverage (0.5 ML), the molecule–substrate interaction became weak because of the increased density of the F gas phase. The molecule–molecule interaction played a decisive role. The presence of the 2D gas phase prevented the contact between the fluorinated fullerene molecules and the Cu(001) surface, and thus, prevented a further loss of F atoms. Thus, a pseudo-stable (12,0)×(1,9) structure of $C_{60}F_n$ was realized. The transformation of this structure to (4,2)×(0,4) is attributed to the formation of a condensed gas phase (F-induced structures) because of the interaction of the additional F atoms with the Cu(001) surface. A continuous growth of the condensed gas phase was observed. This is because all F atoms left the fluorinated fullerene molecule and a well-known (10,6)×(0,4) structure typical for C_{60} growth on the Cu(001) surface was formed. Thus, it has been demonstrated that the adsorption of $C_{60}F_{18}$ on a Cu(001) surface is a multiple stage process and $C_{60}F_{18}$ coverage plays a critical role in the creation of ordered surface structures. The physical and chemical effects resulting from the step-by-step detachment of F atoms from the C_{60} cage might be technologically relevant in nanoscale-localized chemical reactions driven by molecular coverage and practical employment of $C_{60}F_{18}$ molecules as fluorine sources for controllable surface doping applications.

Acknowledgements

We thank Prof. L. N. Sidorov for providing us with $C_{60}F_{18}$ fullerenes. The research has been supported by the Russian Foundation for Basic Research (RFBR) grants (Nos. 16-02-00818-a and 14-02-97022R-Povolzhye-a) and by the computing facilities of the Lomonosov Moscow State University, Research Computing Center. DFT calculations were performed at CSIR-CECRI and SNU facilities. V. K. thanks the Shiv Nadar University High performance computer center Magus.

Electronic Supplementary Material: Supplementary material (sample preparation procedure; simulated STM topographies for different $C_{60}F_{18}$ orientation as well as for $C_{60}F_{12}$ and $C_{60}F_{18}$ molecules on F covered Cu(001) surface; ordering of $C_{60}F_{12}$ molecules within a 2D island; growth of new F-related structures in real-time; transformation of fluorinated fullerene islands over time; effect of low coverage adsorption of $C_{60}F_{18}$ on Cu(001) surface) is available in the online version of this article at https://doi.org/10.1007/s12274-017-1823-9.

References

[1] Ratner, M. A brief history of molecular electronics. *Nat. Nanotechnol.* **2013**, *8*, 378–381.

[2] Loertscher, E. Wiring molecules into circuits. *Nat. Nanotechnol.* **2013**, *8*, 381–384.

[3] Quek, S. Y.; Kamenetska, M.; Steigerwald, M. L.; Choi, H. J.; Louie, S. G.; Hybertsen, M. S.; Neaton, J. B.; Venkataraman, L. Mechanically controlled binary conductance switching of a single-molecule junction. *Nat. Nanotechnol.* **2009**, *4*, 230–234.

[4] Liljeroth, P.; Repp, J.; Meyer, G. Current-induced hydrogen tautomerization and conductance switching of naphthalocyanine molecules. *Science* **2007**, *317*, 1203–1206.

[5] Yee, S. K.; Sun, J. B.; Darancet, P.; Tilley, T. D.; Majumdar, A.; Neaton, J. B.; Segalman, R. A. Inverse rectification in donor–acceptor molecular heterojunctions. *ACS Nano* **2011**, *5*, 9256–9263.

[6] Haddon, R. C.; Perel, A. S.; Morris, R. C.; Palstra, T. T. M.; Hebard, A. F.; Fleming, R. M. C_{60} thin film transistors. *Appl. Phys. Lett.* **1995**, *67*, 121–123.

[7] Kobozono, Y.; Nagano, T.; Haruyama, Y.; Kuwahara, E.; Takayanagi, T.; Ochi, K.; Fujiwara, A. Fabrication of C_{60} field-effect transistors with polyimide and $Ba_{0.4}Sr_{0.6}Ti_{0.96}O_3$ gate insulators. *Appl. Phys. Lett.* **2005**, *87*, 143506.

[8] Pahner, P.; Kleemann, H.; Burtone, L.; Tietze, M. L.; Fischer, J.; Leo, K.; Lüssem, B. Pentacene Schottky diodes studied by impedance spectroscopy: Doping properties and trap response. *Phys. Rev. B* **2013**, *88*, 195205.

[9] Günther, A. A.; Sawatzki, M.; Formánek, P.; Kasemann, D.; Leo, K. Contact doping for vertical organic field-effect transistors. *Adv. Funct. Mater.* **2016**, *26*, 768–775.

[10] Tang, M. L.; Bao, Z. A. Halogenated materials as organic semiconductors. *Chem. Mater.* **2011**, *23*, 446–455.

[11] Taylor, R. Fluorinated fullerenes. *Chem.—Eur. J.* **2001**, *7*, 4074–4083.

[12] Selig, H.; Lifshitz, C.; Peres, T.; Fischer, J. E.; McGhie, A. R.; Romanow, W. J.; McCauley Jr, J. P.; Smith III, A. B. Fluorinated fullerenes. *J. Am. Chem. Soc.* **1991**, *113*, 5475–5476.

[13] Tuinman, A. A.; Mukherjee, P.; Adcock, J. L.; Hettich, R. L.; Compton, R. N. Characterization and stability of highly fluorinated fullerenes. *J. Phys. Chem.* **1992**, *96*, 7584–7589.

[14] Boltalina, O. V.; Abdul-Sada, A. K.; Taylor, R. Hyper-fluorination of [60] fullerene by krypton difluoride. *J. Chem. Soc., Perkin Trans. 2* **1995**, 981–985.

[15] Boltalina, O. V.; Markov, V. Y.; Taylor, R.; Waugh, M. P. Preparation and characterisation of $C_{60}F_{18}$. *Chem. Commun.* **1996**, 2549–2550.

[16] Neretin, I. S.; Lyssenko, K. A.; Antipin, M. Y.; Slovokhotov, Y. L.; Boltalina, O. V.; Troshin, P. A.; Lukonin, A. Y.; Sidorov, L. N.; Taylor, R. $C_{60}F_{18}$, a flattened fullerene: Alias a hexa-substituted benzene. *Angew. Chem., Int. Ed.* **2000**, *39*, 3273–3276.

[17] Tuinman, A. A.; Gakh, A. A.; Adcock, J. L.; Compton, R. N. Hyperfluorination of buckminsterfullerene: Cracking the sphere. *J. Amer. Chem. Soc.* **1993**, *115*, 5885–5886.

[18] Boltalina, O. V.; Lukonin, A. Y.; Pavlovich, V. K.; Sidorov, L. N.; Taylor, R.; Abdul-Sada, A. K. Reaction of [60]fullerene with terbium(IV) fluoride. *Fuller. Sci. Technol.* **1998**, *6*, 469–479.

[19] Edmonds, M. T.; Wanke, M.; Tadich, A.; Vulling, H. M.; Rietwyk, K. J.; Sharp, P. L.; Stark, C. B.; Smets, Y.; Schenk, A.; Wu, Q.-H. et al. Surface transfer doping of hydrogen-terminated diamond by $C_{60}F_{48}$: Energy level scheme and doping efficiency. *J. Chem. Phys.* **2012**, *136*, 124701.

[20] Sque, S. J.; Jones, R.; Goss, J. P.; Briddon, P. R.; Oberg, S. First-principles study of C_{60} and $C_{60}F_{36}$ as transfer dopants for p-type diamond. *J. Phys.: Condens. Matter* **2005**, *17*, L21–L26.

[21] Ouyang, T.; Loh, K. P.; Qi, D. C.; Wee, A. T. S.; Nesladek, M. Chemical bonding of fullerene and fluorinated fullerene on bare and hydrogenated diamond. *Chem. Phys. Chem.* **2008**, *9*, 1286–1293.

[22] Tadich, A.; Edmonds, M. T.; Ley, L.; Fromm, F.; Smets, Y.; Mazej, Z.; Riley, J.; Pakes, C. I.; Seyller, T.; Wanke, M. Tuning the charge carriers in epitaxial graphene on SiC(0001) from electron to hole via molecular doping with $C_{60}F_{48}$. *Appl. Phys. Lett.* **2013**, *102*, 241601.

[23] Tada, T.; Uchida, N.; Kanayama, T.; Hiura, H.; Kimoto, K. Charge-transfer doping by fullerenes on oxidized Si surfaces. *J. App. Phys.* **2007**, *102*, 074504.

[24] Oreshkin, A. I.; Bakhtizin, R. Z.; Murugan, P.; Kumar, V.; Fukui, N.; Hashizume, T.; Sakurai, T. Initial stage of the adsorption of fluorofullerene molecules on Si surface. *JETP Lett.* **2010**, *92*, 449–452.

[25] Bakhtizin, R. Z.; Oreshkin, A. I.; Murugan, P.; Kumar, V.; Sadowski, J. T.; Fujikawa, Y.; Kawazoe, Y.; Sakurai, T. Adsorption and electronic structure of single $C_{60}F_{18}$ molecule on Si(111)-7×7 surface. *Chem. Phys. Lett.* **2009**, *482*, 307–311.

[26] Oreshkin, A. I.; Bakhtizin, R. Z.; Mantsevich, V. N.; Oreshkin, S. I.; Savinov, S. V.; Panov, V. I. STM/STS study of $C_{60}F_{36}$ molecules adsorption on 7×7-Si(111) surface. *JETP Lett.* **2012**, *95*, 666–669.

[27] Fujikawa, Y.; Sadowski, J. T.; Kelly, K. F.; Nakayama, K. S.; Nagao, T.; Sakurai, T. Fluorine etching on the Si(111)-7×7 surfaces using fluorinated fullerene. *Surf. Sci.* **2002**, *521*, 43–48.

[28] Shimizu, T. K.; Jung, J.; Otani, T.; Han, Y.-K.; Kawai, M.; Kim, Y. Two-dimensional superstructure formation of fluorinated fullerene on Au(111): A scanning tunneling microscopy study. *ASC Nano* **2012**, *6*, 2679–2685.

[29] Sun, Y. M.; Liu, Y. Q.; Zhu, D. B. Advances in organic field-effect transistors. *J. Mater. Chem.* **2005**, *15*, 53–65.

[30] Bairagi, K.; Bellec, A.; Chumakov, R. G.; Menshikov, K. A.; Lagoute, J.; Chacon, C.; Girard, Y.; Rousset, S.; Repain, V.; Lebedev, A. M. et al. STM study of $C_{60}F_{18}$ high dipole moment molecules on Au(111). *Surf. Sci.* **2015**, *641*, 248–251.

[31] Lebedev, A. M.; Sukhanov, L. P.; Brzhezinskaya, M. M.; Men'shikov, K. A.; Svechnikov, N. Y.; Chumakov, R. G.; Stankevich, V. G. Experimentally observed orientation of $C_{60}F_{18}$ molecules on the nickel single crystal (100) surface. *J. Surf. Investig.-X-Ray Synch. Neutron Tech.* **2012**, *6*, 833–839.

[32] Horcas, I.; Fernández, R.; Gómez-Rodríguez, J.; Colchero, J.; Gómez-Herrero, J.; Baro, A. WSXM: A software for scanning probe microscopy and a tool for nanotechnology. *Rev. Sci. Instrum.* **2007**, *78*, 013705.

[33] Kresse, G.; Furthmüller, J. Efficient iterative schemes for *ab initio* total-energy calculations using a plane-wave basis set. *Phys. Rev. B* **1996**, *54*, 11169–11186.

[34] Kresse, G.; Hafner, J. *Ab initio* molecular dynamics for liquid metals. *Phys. Rev. B* **1993**, *47*, 558–561.

[35] Kresse, G.; Joubert, D. From ultrasoft pseudopotentials to the projector augmented-wave method. *Phys. Rev. B* **1999**, *59*, 1758–1775.

[36] Blöchl, P. E. Projector augmented-wave method. *Phys. Rev. B* **1994**, *50*, 17953–17979.

[37] Abel, M.; Dmitriev, A.; Fasel, R.; Lin, N.; Barth, J. V.; Kern, K. Scanning tunneling microscopy and X-ray photoelectron diffraction investigation of C_{60} films on Cu(100). *Phys. Rev. B* **2003**, *67*, 245407.

[38] Migani, A.; Illas, F. A systematic study of the structure and bonding of halogens on low-index transition metal surfaces. *J. Phys. Chem. B* **2006**, *110*, 11894–11906.

[39] Tersoff, J.; Hamann, D. R. Theory and application for the scanning tunneling microscope. *Phys. Rev. Lett.* **1983**, *50*, 1998–2001.

[40] Tersoff, J.; Hamann, D. R. Theory of the scanning tunneling microscope. *Phys. Rev. B* **1985**, *31*, 805–813.

[41] Kokalj, A. Electrostatic model for treating long-range lateral interactions between polar molecules adsorbed on metal surfaces. *Phys. Rev. B* **2011**, *84*, 045418.

[42] Li, W.-X.; Stampfl, C.; Scheffler, M. Oxygen adsorption on Ag(111): A density-functional theory investigation. *Phys. Rev. B* **2002**, *65*, 075407.

[43] Stroscio, J. A.; Celotta, R. J. Controlling the dynamics of a single atom in lateral atom manipulation. *Science* **2004**, *306*, 242–247.

[44] Berner, S.; Brunner, M.; Ramoino, L.; Suzuki, H.; Güntherodt, H. J.; Jung, T. A. Time evolution analysis of a 2D solid-gas equilibrium: A model system for molecular adsorption and diffusion. *Chem. Phys. Lett.* **2001**, *348*, 175–181.

[45] Berner, S.; de Wild, M.; Ramoino, L.; Ivan, S.; Baratoff, A.; Güntherodt, H.-J.; Suzuki, H.; Schlettwein, D.; Jung, T. A. Adsorption and two-dimensional phases of a large polar molecule: Sub-phthalocyanine on Ag(111). *Phys. Rev. B* **2003**, *68*, 115410.

[46] Wu, K. H.; Fujikawa, Y.; Nagao, T.; Hasegawa, Y.; Nakayama, K. S.; Xue, Q. K.; Wang, E. G.; Briere, T.; Kumar, V.; Kawazoe, Y. et al. Na Adsorption on the Si(111)-(7×7) surface: From two-dimensional gas to nanocluster array. *Phys. Rev. Lett.* **2003**, *91*, 126101.

[47] Wu, K. H.; Fujikawa, Y.; Briere, T.; Kumar, V.; Kawazoe, Y.; Sakurai, T. Dynamics and nano-clustering of alkali metals (Na, K) on the Si(111)-(7×7) surface. *Ultramicroscopy* **2005**, *105*, 32–41.